

## Physical Properties of the AND-1B Core, ANDRILL McMurdo Ice Shelf Project, Antarctica

F. NIESSEN<sup>1\*</sup>, D. MAGENS<sup>1</sup> & A.C. GEBHARDT<sup>1</sup>

<sup>1</sup>Alfred Wegener Institute for Polar and Marine Research, PO Box 120161, 27515 Bremerhaven, Germany

\*Corresponding author (frank.niessen@awi.de)

**Abstract** - Whole-core physical properties of the AND-1B sediment core were determined on site for initial core characterisation and correlation with seismic modelling to predict target-reflector depth. This was accomplished by the application of a GEOTEK MSCL (multisensor core logger) from which detected parameters were converted to wet bulk density (WBD), P-wave velocity (Vp), and magnetic susceptibility (MS). Due to difficulties in terms of sensor drift, non-contact resistivity (NCR) data were not processed on site. Standards were logged together with the cores throughout the entire depth range to monitor data quality and demonstrate that no systematic offsets occurred between different core diameters of the AND-1B core (PQ-liner, PQ, HQ, and NQ). Physical properties exhibit a large range of values, reflecting the different nature of the various lithologies including clasts, effects of cementation, and overall downcore gradients in WBD and Vp as a result of compaction. Generally, the boundaries of the major stratigraphic units are in good agreement with changes in the pattern of the physical properties. WBD, Vp, and MS exhibit remarkable cyclicities in particular in the upper part of the core down to about 600 metres below seafloor (mbsf).

### INTRODUCTION

Whole-core physical properties provide initial core characterisation with a very high vertical resolution. During the drilling of ANDRILL (AND)-1, on-site core measurements were carried out in a similar way to the previous International Cape Roberts Project (CRP-1 to CRP-3, Cape Roberts Science Team 1998, 1999, 2000) and the on-ice site-survey work for the AND-1 project on the McMurdo Ice Shelf in 2003 (Barrett et al. 2004). In addition, a new sensor was used that enables contact-free determination of electrical resistivity of the core ([www.geotek.co.uk](http://www.geotek.co.uk)).

Physical properties, such as wet bulk density (WBD), P-wave velocity (Vp) and magnetic susceptibility (MS) can be used to define and interpret stratigraphical patterns, including a comparison between lithology and sequences (Niessen & Jarrard 1998; Niessen et al. 1998; Claps et al. 2000; Niessen et al. 2000; Bückler et al. 2001; Naish et al. 2001). In addition, MS can provide evidence for increased volcanism, for example, derived from the McMurdo volcanic province (Niessen et al. 1998). WBD and, in particular, Vp have the potential to indicate post depositional alteration such as by compaction and cementation (Jarrard et al. 2000; Niessen et al. 2000). The P-wave velocities of CRP cores were used to calculate vertical acoustic travel times, which provided the link from seismic profiles to the cores (Henrys et al. 2000, 2001). Thus, linking new data from the AND-1B core to seismic lines will provide further calibration of regional seismic records of the Victoria Land Basin.

During the relatively long drilling season of AND-1 it was important to have available the processed physical-property data soon after each drilling or logging run, because the data were used for making decisions in terms of drilling strategy (Falconer et al. this volume) and for assessment of scientific achievements (Naish et al. this volume). In this paper the terminology of AND-1 refers to cores retrieved from different holes under the AND-1 location on the McMurdo/Ross Ice Shelf, whereas AND-1B refers to the single long core drilled to the final depth of 1284.87 mbsf.

One major goal of measuring physical properties on the AND-1B core at the drill site was using velocity data to assess the depths of seismic reflectors identified as drilling targets. Thus, it was essential to calibrate each logging run individually followed by processing of the raw data, which were then accumulated according to depth and acoustic travel time as drilling proceeded. A full analysis of the quality of calibration and processing was possible only after drilling was finished and all calibration data from different core diameters were available. This analysis and subsequent corrections were made off-ice during the first months after the drilling and are included in this report.

The aims of this paper are to (1) report on data acquisition, calibration and processing of physical properties during the drilling phase on ice, (2) present the analysis of physical-property standards and application of corrections off-ice, and (3) give a preliminary overview of stratigraphic pattern in the physical-property data, effects of diagenesis, and downcore gradients of the AND-1B core.

## METHODS AND MATERIALS

Measurements at the drill-site laboratory included nondestructive, near-continuous determinations of WBD, Vp, NCR raw data, and MS at 1 to 4 centimetre (cm) intervals depending on type of core (mud or rock) and rate of core recovery per shift. The multi sensor core logger (MSCL, GEOTEK Ltd., UK) was used to measure core temperature, core diameter, P-wave travel time, gamma-ray attenuation, electrical conduction, and MS raw data as described in the GEOTEK MSCL manual. As part of the procedure to determine P-wave velocities, data acquisition of full-waveform transmission seismograms followed the approach described in Breitzke et al. (1996). Individual transmission seismograms were digitised using a high-speed ADC board placed into an industrial PC (Dolch, 233 MHz). The technical specifications of the MSCL system as used during AND-1 drilling are summarised in table 1.

Drilling at the AND-1 site revealed both soft sediments recovered as core in liners and consolidated and/or cemented rock core. Thus, the cores were logged in liners or on plastic carriers. The principle of logging cores in liners on the MSCL track is outlined in Weber et al. (1997) and Best & Gunn (1999). The principle of logging cores on carriers is described in detail in the CRP-2 Initial Report (Cape Roberts Science Team 1999). During the AND-1 drilling season

the MSCL had two central sections holding Vp and gamma sensors. The orientation of the P-wave and gamma sensors was horizontal for cores logged in liners and vertical for cores logged on carriers. Except for shorter coring runs, data were logged in continuous intervals of 3 to 18 metres (m) (usually 6 m) long core sections.

For each of these runs, calibration sections (standard cylinders) were logged to calibrate and/or monitor data quality of core diameter, WBD, Vp, and NCR, which is described in more detail below. An empty plastic tube of 0.2 m length was logged to obtain levels of drift of MS and NCR sensors at the end of a logging run. Prior to logging, cores on carriers were described with respect to occurrence of cracks, fractures, and unconsolidated or crumbly materials, which influence physical-property data.

Raw data from single core runs drilled from below seafloor were processed together with raw data measured on calibration and monitoring standard cylinders logged at the top and bottom of each core run. WBD and Vp logs were processed from the raw data using GEOTEK software, which applies data calibration as described below. MS and NCR data remained in raw-data state. From there these data were exported to Kaleidagraph. After run-wise separation of processed calibration data and core data both data sets were accumulated according to depth.

Tab. 1 - Multi sensor Core Logger (MSCL, ser. no. 25) Specifications of AND-1

| <b>P-wave Velocity and Core Diameter</b> |  |
|--|--|
| Sensor orientation                       | Vertical PQ, HQ, NQ, horizontal PQ-liner   |
| Transducer                               | Acoustic Rolling Contact Transducer (ARC) (GEOTEK Ltd.) and Piston Transducer (PT) |
| Transmitter pulse frequency              | 230kHz (ARC), 250kHz (PT)  |
| Transmitted pulse repetition rate        | 100Hz  |
| Received pulse resolution                | 50ns   |
| P-wave travel-time offset [ $\mu$ s]     | 7.13 PQ-liner, 16.9 PQ, 17.6 HQ, 17.2 NQ   |
| <b>P-wave Transmission Seismograms</b>   |  |
| ADC board                                | T3012 (National Instruments)   |
| Sampling frequency and resolution        | 30MHz, 12 bit  |
| Sampling interval                        | 50ns   |
| Length of seismograms                    | 200ms  |
| <b>Wet Bulk Density</b>                  |  |
| Sensor orientation                       | Vertical PQ, HQ, NQ, horizontal PQ-liner   |
| Gamma ray source                         | Cs-137   |
| Source activity                          | 356MBq   |
| Source energy                            | 0.662MeV   |
| Counting time                            | 10s  |
| Collimator diameter                      | 2.5mm  |
| Gamma detector                           | NaI-Scintillation Counter (John Count Scientific Ltd.)                             |
| <b>Magnetic Susceptibility</b>           |  |
| Loop sensor type                         | MS-2B (Bartington Ltd.)  |
| Loop sensor diameter                     | 100mm PQ, 80mm PQ-Liner, HQ, NQ  |
| Alternating field frequency              | 0.565kHz   |
| Sensitivity                              | 10s (<20 $10^{-5}$ SI), 1s (>20 $10^{-5}$ SI)                                      |
| Magnetic field intensity                 | approx. 80A/m RMS  |
| Loop sensor correction coeff. K-rel      | 1.223 PQ-Liner, 1.487 PQ   |
| Loop sensor correction coeff. K-rel      | 1.1795 HQ, 0.4848 NQ   |
| <b>Temperature and Resistivity</b>       |  |
| Sensor types                             | Infrared and NCR   |

Core data were corrected for depth below seafloor where appropriate. Using Kaleidagraph's graphical editor, WBD, Vp, and MS core data were cleaned run-wise for odd data points related to core destruction (naturally or coring induced, gaps on carriers or between carriers) or obvious malfunction of MSCL data acquisition. At levels of low MS ( $0-10 \times 10^{-5}$  SI), linear sensor-drift corrections were applied where appropriate, in order to clean negative values from the data. Calculation of fractural porosity and correction of MS were carried out after cleaning the data.

## WHOLE-CORE PHYSICAL-PROPERTY DETERMINATION

### MAGNETIC SUSCEPTIBILITY (MS)

MS was measured in terms of SI units corrected for loopsensor and core diameter as follows:

$$\text{MS} (10^{-5} \text{ SI}) = \text{measured value} (10^{-5} \text{ SI}) / K\text{-rel} \quad (\text{i})$$

K-rel is a sensor-specific correction calculated from the diameter of the core over the diameter of the loop sensor as outlined in the GEOTEK MSCL manual and summarised in table 1. The geometry of the loop sensor does not allow a direct determination of volume MS. Data corrected for loop sensor and core diameter can be converted to volume MS by the following equation:

$$\text{Vol-MS} (10^{-5} \text{ SI}) = \text{MS} \times 0.93053 + 2.8986 \quad (\text{ii})$$

This linear regression was determined empirically by plotting the volume susceptibility measured on core plugs (sampled from the matrix of the AND-1B split core; Wilson & Florindo this volume) to whole-core MS at the same depth after removing loop data obviously influenced by magnetic signature of clasts. The remaining matrix MS data revealed a correlation coefficient of 0.984 using 1034 data points (Fig. 1). The whole-core MS data presented here are corrected only with respect to equation (i) and thus directly comparable to the whole-core physical property data presented in the CRP Initial Reports (Cape Roberts Science Team 1998, 1999, 2000).

### P-WAVE VELOCITY (VP)

Vp was measured using two different types of transducers. Cores in liners were logged with standard GEOTEK piston transducers in horizontal orientation. Acoustic coupling between transducers and liner was encouraged by water. For cores on carriers, acoustic rolling contact transducers (ARC, GEOTEK Ltd., UK) were used. These transducers were rolling along the top of the core (upper transducer) and the bottom outside of the carrier (lower transducer), respectively. Vp was calculated from the core diameter and travel time after subtraction of the P-wave travel time through the core carrier (or core liner) wall, transducer, electronic delay, and detection offset between the

first arrival and second zero-crossing of the received waveform (P-wave travel-time offset, or PTO), where the travel time can be best detected (Cape Roberts Science Team 1998, 1999, 2000). This travel-time offset was determined using cylindrical plastic standards of PQ, NQ, and HQ core size of known velocities ( $2330 \text{ ms}^{-1}$  for PQ and HQ and  $2382 \text{ ms}^{-1}$  for NQ). For PQ-core in liner we used a liner filled with water and plastic standard to calibrate and monitor velocity. Vp values were normalised to  $20^\circ\text{C}$  using the temperature logs. Core temperature was measured using a calibrated infrared sensor:

$$V_p = V_{pm} + 3 \times (20 - t_m) \quad (\text{iii})$$

where  $V_{pm}$  = P-wave velocity at measured temperature;  $t_m$  = measured temperature.

### FULL-WAVEFORM TRANSMISSION SEISMOGRAMS

In addition to the standard Vp-detection system of the GEOTEK MSCL, a laboratory-built full P-wave registration apparatus was used to digitise and store transmission seismograms. We used the same approach and apparatus as described for physical-properties logging of the Cape Roberts Project (Cape Roberts Science Team 1999, 2000). Data were stored for further post-drilling analysis. During the AND-1 drilling season the system did not allow other than computer-screen visualization. The analysis of seismograms is part of the off-ice research.

### CUMULATIVE TWO-WAY TRAVEL TIME

Vp measured across the core at a given depth interval was used to calculate the vertical travel time in the core to the next deeper interval, thereby assuming isotropy of the materials on scales of a few centimetres. During the drilling phase, these travel times between depth intervals were compiled to a

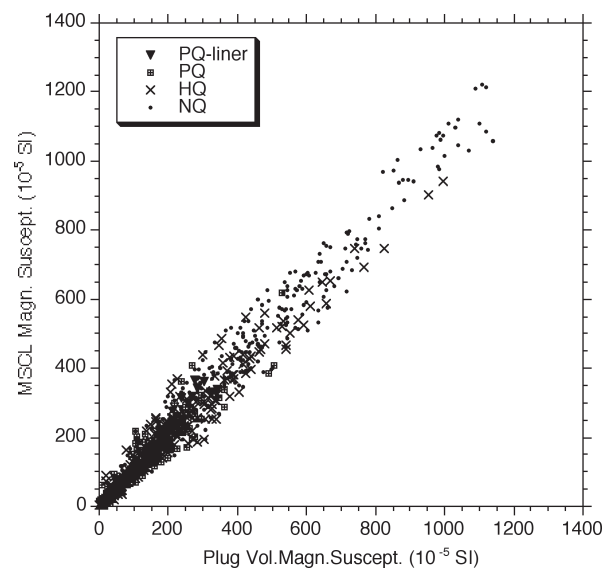


Fig. 1 – Correlation of MSCL magnetic susceptibility (corrected for different loop and core diameter) and volume magnetic susceptibility of plug samples analysed by the Palaeomagnetic Group on ice (Wilson et al. this volume).

cumulative two-way travel time to depth conversion in order to predict the depths of the target reflectors defined on the seismic profile. Velocities of the AND-1B core were not corrected for borehole conditions in terms of *in situ* pressure and temperature. The application is described in more detail in Morin et al. (this volume) and will be included in off-ice science reporting and publication.

### WET BULK DENSITY (WBD)

WBD was determined from attenuation of a gamma-ray beam transmitted from a radioactive source ( $^{137}\text{Cs}$ ). A beam collimator of 2.5 millimetres (mm) was used and the beam was focused through the core-centre into a gamma detector. For density calibration, standard core-size cylinders consisting of different proportions of aluminium and water were used.

For PQ-liner we used a set of aluminium plates of different thickness (ranging from 0 mm to full core size) placed in a liner filled with water as described in Best & Gunn (1999). A reversed arrangement of core-size aluminium containers filled with different volumes of water was used for PQ, HQ, and NQ core on carriers (Fig. 2). The calibration cylinders were manufactured by AWI and have three sections. One section is aluminium only. The other two sections contain cylindrical chambers of different volumes cut into the central part of the aluminium core and sealed. Through a valve, the chambers can be filled with water (Fig. 2). For cores logged on carriers this is the only way to ensure that the different gamma-ray absorption coefficients of solid material (minerals or aluminium) and water are considered for calibration (Weber et al. 1997). This is a prerequisite for densities of solid porous materials (like the AND-1B core) being determined correctly. To our knowledge, this procedure has been used first during AND-1B drilling. For the CRP cores, for example, only solid calibration cylinders

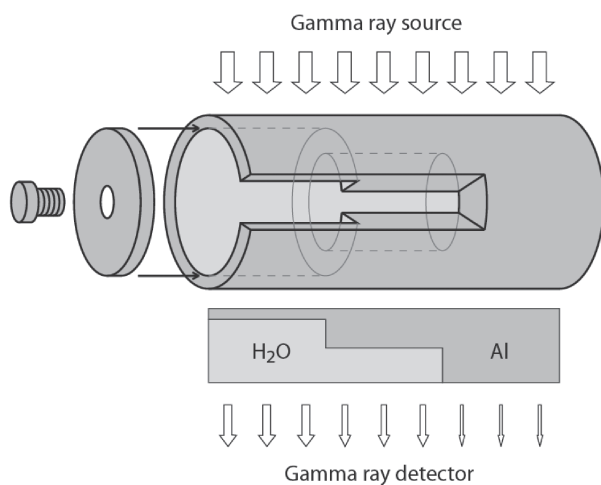


Fig. 2 – The shape and principle of aluminium cylinders used for WBD calibration from gamma-ray attenuation. The containers had PQ, HQ, and NQ outer diameters, were filled with distilled water, and were logged on carriers.

were used, including aluminium and plastic (Cape Roberts Science Team 1998, 1999, 2000). During AND-1B drilling the aluminium calibration cylinders were logged at the end of each PQ, HQ, and NQ core-logging run. In addition, a plastic cylinder of known density was logged at the top and bottom end of each run for monitoring purposes.

To calibrate WBD from gamma counts, we used the approach by Best & Gunn (1999), also described in the GEOTEK-MSCL manual, which applies a second-order polynomial function to describe the relationship between the natural logarithm of gamma counts per second (ln cps) and the product of density and thickness of the measured material. For calibration the equations are determined empirically for different core size on each run by plotting average data points of water only, aluminium only, and, for materials on carrier, different proportions of water and aluminium (Fig. 3).

### FRACTIONAL POROSITY (POR)

Based on MSCL logging, fractional porosity is not an independent data-acquisition parameter but can be calculated from the WBD as follows:

$$\text{POR} = (\text{dg} - \text{WBD}) / (\text{dg} - \text{dw}) \quad (\text{iv})$$

where dg = grain density ( $2.7 \text{ g cm}^{-3}$ ); dw = pore-water density ( $1.03 \text{ g cm}^{-3}$ ).

This approach makes the assumption that grain density and pore-water density are constant. This is not the case for the AND-1B core. Pore water has been analysed as part of the on-ice work and ranges from 28‰ to 58‰ (S. Vogel personal communication), which corresponds to densities from  $1.023 \text{ g cm}^{-3}$  to  $1.046 \text{ g cm}^{-3}$ , respectively. Therefore, using  $1.03 \text{ g cm}^{-3}$  as constant pore-water density provides a reasonable approximation. However, grain density is expected to be a lot more variable in different lithologies, ranging from diatomites to large single rock clasts or volcanic intrusions. Grain densities are analysed in discrete samples as part of the off-ice science. Thus, determination of porosity from whole-core logging

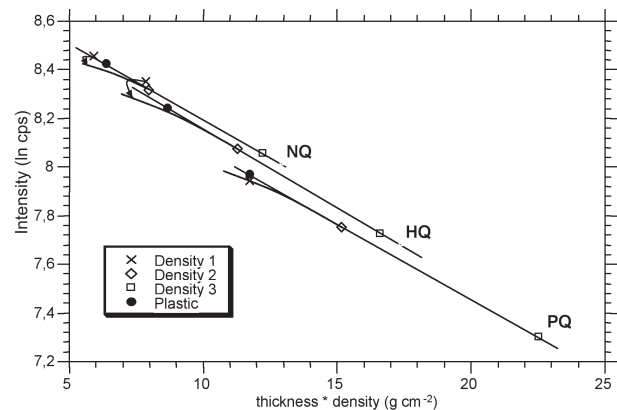


Fig. 3 – Gamma-ray attenuation (ln cps) plotted versus thickness times density of PQ, HQ, and NQ calibration cylinders. 'Density 1 and 2' refer to different proportions of distilled water and aluminium. 'Density 3' is aluminium only (see Fig. 2 for illustration). 'Plastic' refers to full plastic cylinders of PQ, HQ, and NQ size.

will be presented in a forthcoming research paper in more detail. The equation above may be used for a rough preliminary approximation of porosity only.

### NON-CONTACT RESISTIVITY (NCR)

For the first time our MSCL was equipped with a GEOTEK non-contact electrical resistivity sensor (NCR). The NCR technique operates by inducing a high-frequency magnetic field in the core, from a transmitter coil, which in turn induces electrical currents in the core. The latter are inversely proportional to the resistivity. Subsequently, very small magnetic fields regenerated by the electrical current are measured by a receiver coil. To measure these very small magnetic fields accurately, a difference technique has been developed that compares the readings generated from the measuring coils to the readings from an identical set of coils operating in air. Resistivities between 0.1 and 10 ohm-metres can be measured at spatial resolutions along the core of approximately 2 cm.

Raw data are expressed in [mV] and indicate the conductivity of the core. For converting raw data to resistivity, calibration containers with brines of known resistivities have to be logged. After each core-logging run, we logged five 0.3 m-long containers with an internal diameter close to that of the core filled with water of known salinities (0.35‰, 1.75‰, 3.5‰, 17.5‰, and 35‰). The calibration is described in the GEOTEK MSCL manual. In the field, no calibration was applied as the raw data indicated strong data drift after zeroing, which included the calibration containers.

### DATA QUALITY CONTROL AND OFF-ICE CORRECTIONS

Vp and WBD data of all calibration and control pieces (standard cylinders) were compiled, divided into the different core diameters from PQ-liner to NQ, statistically analysed, and compared to the known reference values (Tab. 1). Generally, the standard deviation is low and the means of the standards derived from MSCL measurements fit very well to the respective reference values. We applied minor corrections to the Vp data and a larger correction to WBD data of HQ core size.

### VP DATA CORRECTION

For each core diameter (PQ, HQ, or NQ) the mean of Vp data determined on standard cylinders were compared to the reference values. The deviations were used to correct Vp section-wise (monitoring and core data) as follows: PQ: +74 m s<sup>-1</sup>, HQ: +19 m s<sup>-1</sup>, NQ to a depth of 1 074 mbsf: +8 m s<sup>-1</sup>, NQ for depth deeper than 1074 mbsf: -16 m s<sup>-1</sup>. The reason for this correction is that, during drilling, a preliminary PTO (see 'P-wave Velocity' above) was

determined from the calibration data after a few runs of a given core diameter and then used for the entire data of this diameter. On ice there was no time for improving the statistics on the PTO and applications of corrections.

For PQ-liner, and using a PTO based on calibration with water (Tab. 1), the measured plastic standard revealed a significant deviation from the reference Vp value. Because we are not exactly aware of the reasons (different setting compared to PQ, HQ, NQ carrier as the plastic is glued into the liner of which the overall geometry is not precisely known) we preferred to use water of known velocity (and PTO) as P-wave standard for PQ-liner (Tab. 1).

### WBD DATA CORRECTION

After analysis of WBD calibration cylinders of different core size, deviations at the lowest densities between the different core sizes NQ, HQ, and PQ became obvious (Fig. 3). For each core diameter and standards the plot of thickness times density versus intensity (ln CPS) should form similar almost linear or slightly curved relationships (Fig. 3). For PQ it is not surprising that 'Density 1' (the largest volume of water) exhibits lower count intensities than plastic of the same thickness times density, because water has a higher gamma-ray absorption coefficient than solid material (Weber et al. 1997). Therefore, a slightly downward curved line (second-order polynomial, dashed line as plotted for PQ) is more reasonable than a straight line linking 'Density 1 to 3' and 'Plastic' (Fig. 3). However, the difference between 'Density 1' and 'Plastic' is small and negligible considering the total range of errors (Fig. 4).

A strong positive deviation of 'Density 1' is observed for all HQ runs (Fig. 3). The gamma-ray intensity of 'Density 1' is a lot higher than it should be compared to PQ and NQ. The most probable explanation is trapped air in the first chamber of the calibration cylinder, which leads to a significant increase of count intensity. We assume (and we observed) that water in the HQ aluminium cylinder expanded and contracted as reaction to temperature fluctuations at the drill-site laboratory. As a consequence, water was squeezed out during expansion through a damaged seal. Subsequently air was sucked into the water chamber during contraction. Although not visible, the air would form a bubble along the top of the largest water chamber. Thus, due to the circular shape of the container lying on the MSCL track and the vertical orientation of the beam, only the largest water chamber is affected by trapped air. Apparently, this effect has not occurred for the PQ standard cylinder and perhaps to a minor extent for the NQ cylinder, because here 'Density 1' is exactly on the line with 'Plastic' but should have slightly lower counts (Fig. 3).

Since the WBD of HQ core size was calibrated on ice using 'Densities 1 to 3' (Fig. 3), on-ice data have a significant bias at low to medium densities. In order

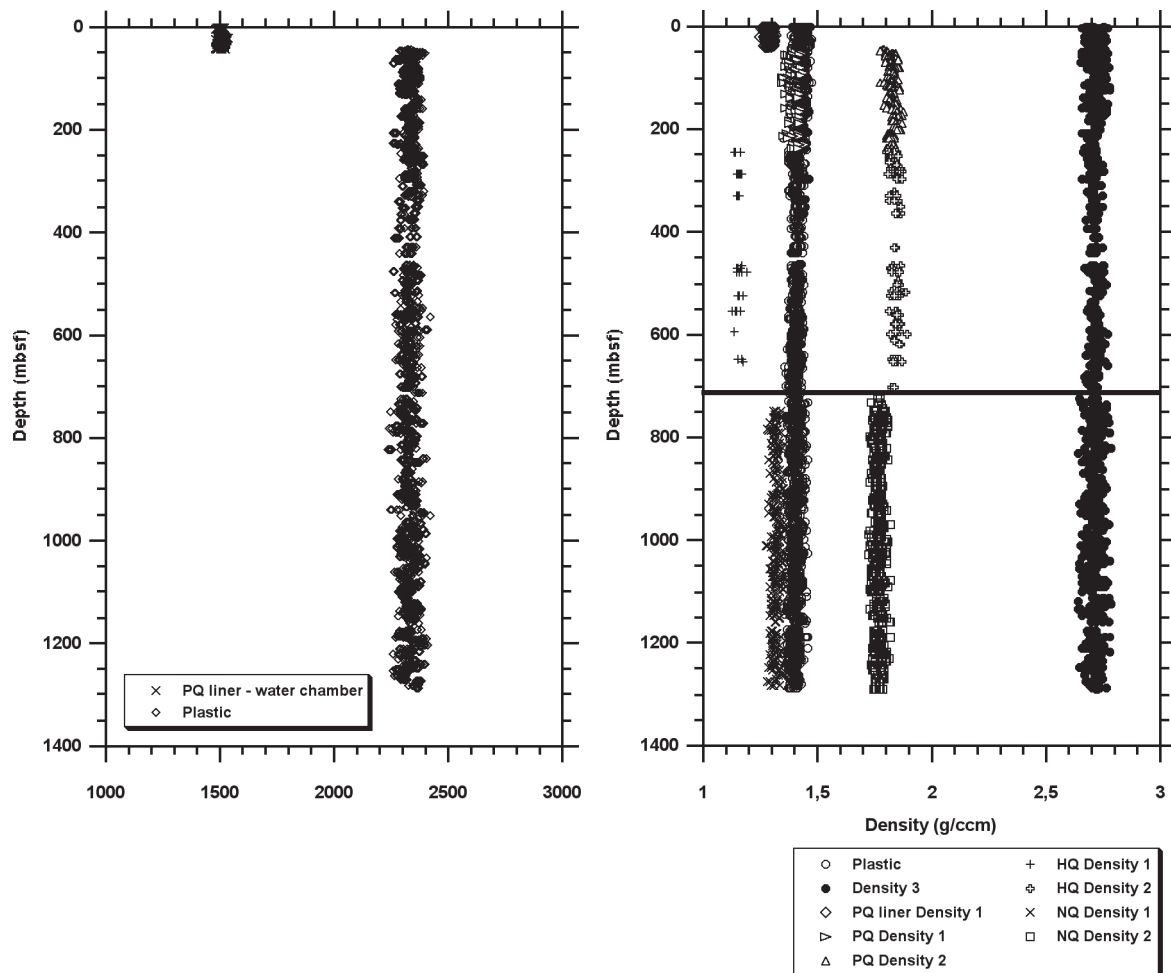


Fig. 4 – Vp and WBD determined on standard cylinders logged together with core runs from AND-1B. The different standards are listed in table 2. Note that depths values are assigned in dependent on the respective run depth of core, so they are fictive values. This explains an overlap of the diameter-specific symbols at diameter boundaries, since depth information of initial calibration pieces before the first sediment section may show similar values to those of standard cylinder at the end of the respective previous run.

to correct for this bias, selected runs covering the entire range of densities of HQ core were reprocessed off-ice by only using 'Densities 2 and 3' plus plastic. The resulting data set was statistically compared to the original. A second-order polynomial function was applied to correct all of the original HQ density data accordingly.

The systematic offset in intensity observed between PQ, HQ, and NQ calibration lines (Fig. 3) can be explained by the behaviour of the GEOTEK gamma detector (Weber et al. 1997), which has an offset if similar materials are measured at different count rates (for example, because of different diameters). This offset has no effect on data quality as each core diameter has been treated separately and individually.

### PRELIMINARY RESULTS AND INTERPRETATION

On core AND-1B, a total of 74 190 lines of physical property data were produced. These data will allow a general characterisation of the core material and provide a large potential for further analyses, which require a high vertical resolution. Together with the

core, a total of 5781 lines of physical property data were determined on standard calibration cylinders for monitoring data quality (Fig. 4). Because the core was drilled in four different diameters it is important to analyse the data of the standards for systematic offsets between the diameters as such offsets would also be present in the core data.

### DOWNCORE MONITORING OF STANDARDS

Vp and WBD standards are plotted versus depth (Fig. 4) for providing insight into the behaviour of the standards over the whole logging period and thus depth range of the core (Fig. 4).

Standard values for aluminium ('Density 3') and 'Plastic' vary in a certain range downcore but do not show a certain 'downcore' trend (Fig. 4), which ensures the core data have no offset between different core diameters. By comparison with the total range in sediment parameter values of both Vp and WBD (Fig. 5) it becomes evident that the fluctuation of standard data points is negligibly small. Systematic offsets in the Vp plastic standard between PQ and HQ/NQ are due to the fact that the white plastic for PQ has a slightly different reference velocity as the black plastic standard used for HQ

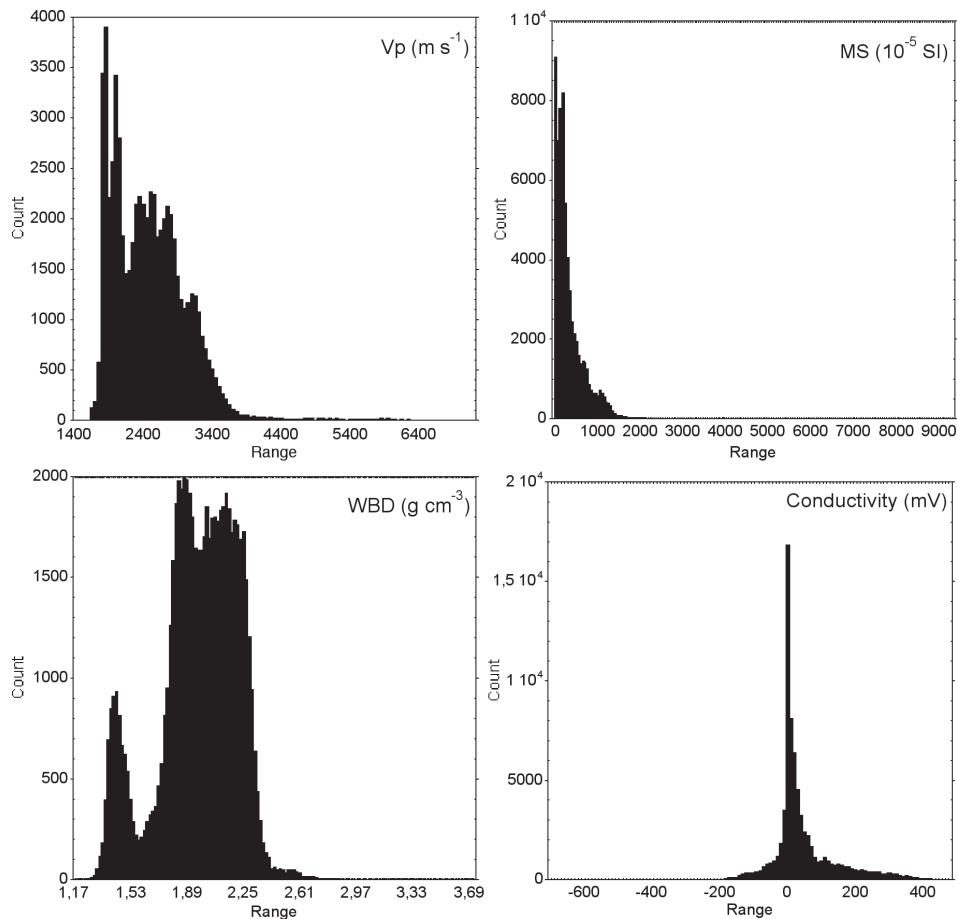


Fig. 5 – Histograms of all physical-property data of core AND-1 and -1B. Data are based on 64 202 (Vp), 66 630 (WBD) and 73 859 (MS and NCR-conductivity) measurements. Note that 9657 and 7229 data points were eliminated during cleaning from original Vp and WBD data, respectively. Eliminated data are not shown.

and NQ (Fig. 4). The small offset is therefore a function of the material rather than core size.

Also, offsets between 'Densities 1 and 2' between the different core diameters of PQ liner to NQ (Fig. 5) are due to the fact that they do not have the same reference density (see Tab. 2 for comparison). It is noticeable that the range of standard data points is least for HQ. One reason is that the core thickness determination was most stable for HQ (lowest standard deviation on calibration pieces; Tab. 1), while, for no particular reason, slightly higher variability was observed for the other core diameters. Measured core diameters are used for WBD processing using GEOTEK software.

#### CORE DATA RANGES, STATISTICS AND TRENDS

Vp ranges from 1460 m s<sup>-1</sup> in unconsolidated mud at the top of the core to more than 7000 m s<sup>-1</sup> in large single clasts. The distribution of Vp is slightly negative-skewed and bimodal (Fig. 5). The former effect is mostly due to very high Vp measured in clasts of core size or bigger, which do not occur very frequently in the record. Some high velocities may also be related to cementation. Bimodality is related to the cyclic behaviour of the core between mudstones and diatomites (low Vp) and the rest of

the core including thick diamictites (higher velocities). There is an overall linear downcore gradient in Vp from 1791 m s<sup>-1</sup> at the top to 3188 m s<sup>-1</sup> at the bottom of the core.

WBD ranges from about 1.4 g cm<sup>-3</sup> and less in mudstones, diatomites and pumice to up to about 3.7 g cm<sup>-3</sup> in large clasts. The distribution is bimodal for similar reasons as described above for Vp. The positive tail is not so distinct as in Vp data (Fig. 5). For clasts having higher densities than 2.7 g cm<sup>-3</sup> negative fractional porosities are calculated because the actual density is higher than assumed for processing porosity from density according to equation (iv). There is an overall downcore gradient in WBD from 1.76 g cm<sup>-3</sup> at the top to 2.26 g cm<sup>-3</sup> at the bottom of the core. Accordingly, preliminary fractional porosity exhibits a negative trend from 0.56 at the top to 0.26 at the bottom of the core.

MS resolved significant variability over four orders of magnitude. MS below 10 (10<sup>-5</sup> SI) is frequently observed in diatomites and some large clasts. MS data are mostly below 2000 (10<sup>-5</sup> SI) but in volcanic clasts and volcanic rocks values can reach up to about 9000 (10<sup>-5</sup> SI). Thus, the distribution is strongly negative-skewed (Fig. 5) and data should be plotted on a logarithmic scale, in order to visualise downcore variability at lower MS, in particular in diatomites (Fig. 5). There are large MS fluctuations in the core

Tab. 2 - Compilation of reference values and MSCL measurements of standard cylinders.

| Standard material          | Type of standard                | Core diameter | Reference value | No. of measuring points on standards | Min. | Max. | Mean | Std. Deviation |
|----------------------------|---------------------------------|---------------|-----------------|--------------------------------------|------|------|------|----------------|
| Alumin.-water mixture      | Density 1 (g cm <sup>-3</sup> ) | PQ liner      | 1.28            | 224                                  | 1.25 | 1.31 | 1.28 | 0.01           |
| Alumin.-water mixture      | Density 2 (g cm <sup>-3</sup> ) | PQ liner      | 1.49            | 241                                  | 1.45 | 1.55 | 1.50 | 0.01           |
| Alumin.-water mixture      | Density 3 (g cm <sup>-3</sup> ) | PQ liner      | 1.72            | 252                                  | 1.66 | 1.77 | 1.73 | 0.02           |
| Alumin.-water mixture      | Density 4 (g cm <sup>-3</sup> ) | PQ liner      | 1.93            | 222                                  | 1.88 | 1.98 | 1.94 | 0.02           |
| Alumin.-water mixture      | Density 5 (g cm <sup>-3</sup> ) | PQ liner      | 2.14            | 242                                  | 2.10 | 2.19 | 2.14 | 0.02           |
| Alumin.-water mixture      | Density 6 (g cm <sup>-3</sup> ) | PQ liner      | 2.34            | 268                                  | 2.30 | 2.39 | 2.34 | 0.02           |
| Alumin.-water mixture      | Density 7 (g cm <sup>-3</sup> ) | PQ liner      | 2.52            | 259                                  | 2.48 | 2.59 | 2.54 | 0.02           |
| Aluminum                   | Density 8 (g cm <sup>-3</sup> ) | PQ liner      | 2.71            | 139                                  | 2.66 | 2.76 | 2.72 | 0.02           |
| Plastic (white)            | Density (g cm <sup>-3</sup> )   | PQ liner      | 1.41            | 135                                  | 1.38 | 1.47 | 1.43 | 0.02           |
| Water (in liner container) | Velocity (m s <sup>-1</sup> )   | PQ liner      | 1470            | 942                                  | 1476 | 1533 | 1492 | 9.6            |
| Plastic (white)            | Velocity (m s <sup>-1</sup> )   | PQ liner      | 2382            | 146                                  | 1787 | 2321 | 2236 | 116.6          |
| Aluminum-filled liner      | Diameter (cm)                   | PQ liner      | 6.63**          | 119                                  | 6.62 | 6.64 | 6.63 | 0.004          |
| Alumin.-water mixture      | Density 1 (g cm <sup>-3</sup> ) | PQ            | 1.41            | 146                                  | 1.34 | 1.45 | 1.40 | 0.02           |
| Alumin.-water mixture      | Density 2 (g cm <sup>-3</sup> ) | PQ            | 1.82            | 221                                  | 1.77 | 1.87 | 1.82 | 0.02           |
| Aluminum                   | Density 3 (g cm <sup>-3</sup> ) | PQ            | 2.71            | 212                                  | 2.65 | 2.78 | 2.71 | 0.03           |
| Plastic (white)            | Density (g cm <sup>-3</sup> )   | PQ            | 1.41            | 713                                  | 1.35 | 1.47 | 1.42 | 0.02           |
| Plastic (white)            | Velocity (m s <sup>-1</sup> )   | PQ            | 2382            | 812                                  | 2308 | 2448 | 2382 | 24.7           |
| Plastic (white)            | Diameter (cm)                   | PQ            | 8.3             | 841                                  | 8.19 | 8.47 | 8.31 | 0.03           |
| Alumin.-water mixture      | Density 1 (g cm <sup>-3</sup> ) | HQ            | 1.28            | 40                                   | 1.12 | 1.19 | 1.15 | 0.01           |
| Alumin.-water mixture      | Density 2 (g cm <sup>-3</sup> ) | HQ            | 1.84            | 117                                  | 1.80 | 1.89 | 1.84 | 0.02           |
| Aluminum                   | Density 3 (g cm <sup>-3</sup> ) | HQ            | 2.71            | 286                                  | 2.66 | 2.77 | 2.71 | 0.02           |
| Plastic (black)            | Density (g cm <sup>-3</sup> )   | HQ            | 1.41            | 701                                  | 1.36 | 1.46 | 1.41 | 0.02           |
| Plastic (black)            | Velocity (m s <sup>-1</sup> )   | HQ            | 2328            | 777                                  | 2257 | 2418 | 2329 | 26.4           |
| Plastic (black)            | Diameter (cm)                   | HQ            | 6.12            | 789                                  | 6.09 | 6.17 | 6.12 | 0.01           |
| Alumin.-water mixture      | Density 1 (g cm <sup>-3</sup> ) | NQ            | 1.30            | 267                                  | 1.27 | 1.37 | 1.32 | 0.02           |
| Alumin.-water mixture      | Density 2 (g cm <sup>-3</sup> ) | NQ            | 1.76            | 525                                  | 1.72 | 1.82 | 1.76 | 0.02           |
| Aluminum                   | Density 3 (g cm <sup>-3</sup> ) | NQ            | 2.71            | 499                                  | 2.64 | 2.78 | 2.71 | 0.03           |
| Plastic (black)            | Density (g cm <sup>-3</sup> )   | NQ            | 1.41            | 1139                                 | 1.34 | 1.46 | 1.40 | 0.02           |
| Plastic (black)            | Velocity (m s <sup>-1</sup> )   | NQ            | 2328            | 1213                                 | 2235 | 2416 | 2328 | 31.2           |
| Plastic (black)            | Diameter (cm)                   | NQ            | 4.5             | 1227                                 | 4.43 | 4.58 | 4.50 | 0.02           |

\*\* Reference diameter refers to inner diameter of the liner. The outer diameter of 7.13 cm (standard liner diameter) is measured during logging procedure and corrected for the thickness of the liner wall (0.508 cm) during data processing assuming constant

but no significant overall down-core trend in the data.

The NCR sensor is a relatively new product of GEOTEK, and the drill-site logging team had no experience with using this sensor at the beginning of the drilling phase. NCR raw data ranges from +500 mV in relatively well conducting materials to -700 mV. The data distribution is nearly Gaussian with a slightly stronger positive tail (Fig. 5). Negative values are artefacts and have to be eliminated or corrected. The raw data are strongly influenced by core size with a larger effect when changing from PQ to HQ than from HQ to NQ. Most negative values were detected in NQ cores. Because negative NCR data cannot be processed using the GEOTEK software, all NCR data are still in the raw state. It is essential to correct for sensor drift or other reasons responsible for negative values prior to processing. A careful analysis is needed to understand the observed effects, because drift can be linear, nonlinear, or absent. Also, other effects like those from room and core temperatures as well as core disturbance (cracks, fractures) need to be analysed. Some of the observed effects also have to be discussed with the manufacturer GEOTEK. For the reasons given above there is only a very small amount of NCR data presented in this report where the data had no drift (Fig. 6).

#### DATA VARIABILITY ON A SELECTED DEPTH INTERVAL OF LSU-2

A depth interval of 6 m in lithostratigraphic unit (LSU) 2.4 (volcanic sandstone, siltstone, and mudstone) is chosen as an example to demonstrate how the different physical properties can vary between different lithologies but also within specific lithologies (Fig. 6). In clayey siltstone and silty claystone (130 to 133 mbsf) Vp, WBD, and MS remain relatively uniform, whereas NCR raw data exhibit a number of distinct cycles not (or not so clearly) resolved in the other properties. In the sandstone-dominated lithologies below 133 mbsf, Vp and WBD become more variable and increase towards the bottom of the section (siltstone), in particular MS, which increases from about 100 to 1000 (10<sup>-5</sup> SI). Once again, the most remarkable cyclic pattern is notable in the NCR data. Most of this variability is probably related to differences in particle size and composition. MS demonstrates that the content of magnetic minerals within volcanically derived units can be quite different on small vertical scales. In addition, NCR data may also be related to fractures because fractures can create extra pathway for fluid flow (including drilling fluid), which increases conduction.

Four thin intervals exhibit contrasting physical

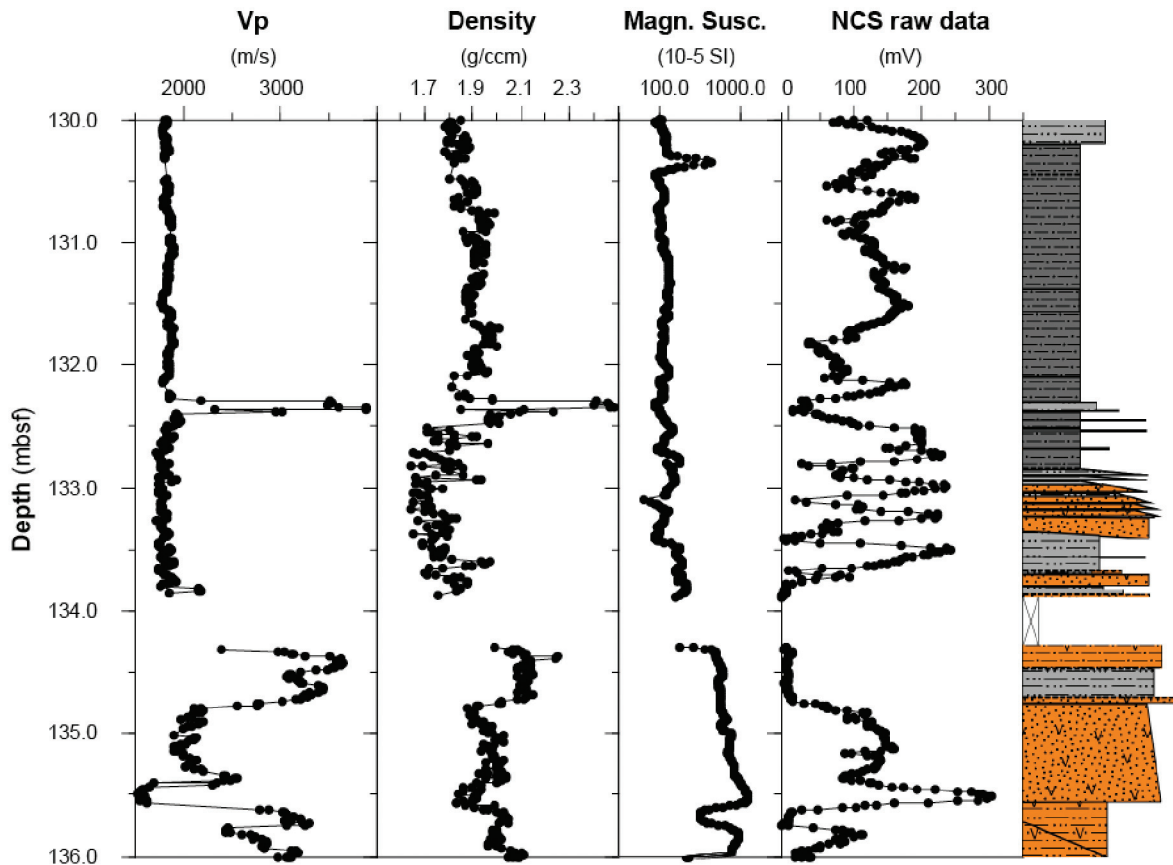


Fig. 6 – Logs of Vp, WBD, MS, and NCR (raw data expressed as conduction in mV) from 130 to 136 mbsf compared to lithology.

properties, which suggest characteristics other than compositional influence the values. Two layers, both containing clasts (clayey siltstone, 132.28 to 132.36 mbsf and mudstone, 134.48 to 134.72 mbsf), and the top of siltstone (135.59 to 135.75 mbsf) have high to very high Vp and WBD, and no change in MS but very low (almost zero) values in NCR. In contrast, the bottom of the graded sandstone (135.77 to 135.59 mbsf) has minimum VP, medium WBD and maximum MS and NCR. These patterns are suggested as being caused by different degrees of cementation. Cementation would not only increase WBD but also change or block the connection of pores, and thereby increase compression and shear modulus, which are positively related to Vp. Blocking of pore connections, may also explain zero NCR values because the data suggest these intervals are not conducting. The opposite is true for the base of the graded sandstone. Weakly cemented or loose sand provides connecting pore space thereby reducing Vp and increasing conduction.

#### PHYSICAL PROPERTIES OF THE ENTIRE CORE AND-1 AND-1B

In order to give an overview of the physical properties of the entire core, WBD, Vp, and MS data were smoothed over 50 data points. In this data the effect of clasts causing higher density and velocity is included, but due to smoothing, single clasts are no longer visible in the graphs (Figs. 7 & 8), unlike the

original data. In most cases the changes in pattern of physical properties is in good agreement with the boundaries of the major stratigraphic units (Figs. 7 & 8; LSU-1 to LSU-8; Krissek et al. this volume). A more careful comparison of lithology and physical properties will be carried out during the off-ice work of the project. Here only a few general observations are described.

Remarkable features of LSU-1 are a step downcore gradient to high WBD of  $2.2 \text{ g cm}^{-3}$  at the bottom of the unit and relatively high Vp of up to  $3000 \text{ m s}^{-1}$  (Fig. 7). The unusual high values in these relatively young and shallow rocks (mostly diamictites) suggest a combination of both subglacial overconsolidation and cementation. LSU-2 is very variable as described in more detail in the example above. WBD is generally lower than in LSU-1, but Vp frequently reach very high values in well-cemented units. LSU-3 is remarkably cyclic with very low WBD down to about  $1.4 \text{ g cm}^{-3}$  in the diatomites alternating with units of higher WBD of up to  $2.4 \text{ g cm}^{-3}$ , most of which are diamictites. In general, Vp is quite low, in particular in diatomites, with the exception of a few diamictites reaching velocities of up to  $3500 \text{ m s}^{-1}$ . The latter is likely to be related to cementation. MS is lower on average than in overlying units mostly caused by very low content of magnetic particles in diatomites. LSU-4 remains cyclic in WBD, Vp, and MS with some spikes of increased density and velocity superimposed on the cycles. Since the spikes are most pronounced in Vp data, once again cementation

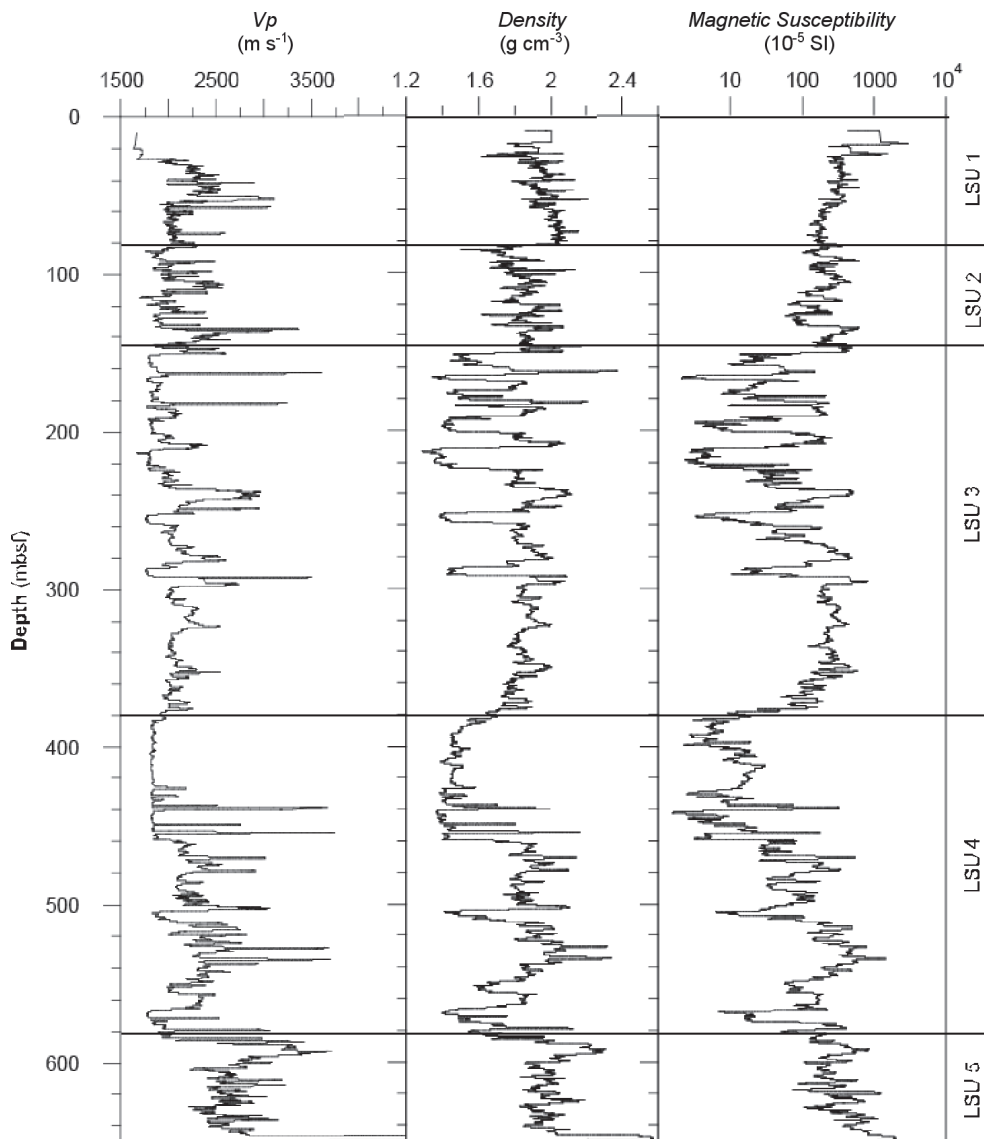


Fig. 7 – Summary logs of Vp, WBD, and MS (cumulative data smoothed over 50 data points) from 0 to 650 mbsf subdivided into lithostratigraphic units (LSU).

could have altered the rocks in some intervals more than in other intervals. MS exhibits a general trend from about 10 to 1000 ( $10^{-5}$  SI) towards the bottom of the unit.

At the top of LSU-5 the largest change in the general pattern of physical properties of the entire core is observed. One feature changing downcore is the much smaller amplitude in fluctuations or cycles in both WBD and Vp, whereas MS maintains a more cyclic pattern down to the bottom of the core (Figs. 7 & 8). The other feature is a sharp downcore onset to higher WBD and Vp at the top of LSU-5. Also remarkable in LSU-5 is the phonolithic lava (646.49 to 649.3 mbsf), which is characterised by very high densities of 2.5 to 2.7  $\text{g cm}^{-3}$  and velocities up to 5500  $\text{m s}^{-1}$ . MS also increases in the lava to more than 4000 ( $10^{-5}$  SI). The boundary between LSU-5 and LSU-6 is not correlated with major changes in the physical properties. A major decrease in WBD and MS and a small decrease in Vp are observed a few metres below the boundary between LSU-6 and LSU-7. The decrease in density in LSU-7 is mainly responsible

for creating a major reflector in the seismic profile, which is the 'bilious green reflector', the final depth target of AND-1B drilling project. The relatively steep velocity gradient in the diamictites of LSU-5 (Fig. 8) is mainly responsible for finding this reflection horizon slightly deeper than expected from the initial velocity model based on stacking velocities (Morin et al. this volume). A return to higher MS as well as Vp and WBD is observed at the onset of LSU-8. The latter may be responsible for the strong double reflector that characterises 'Surface C' in seismic profiles from the area of investigation.

## CONCLUDING REMARKS

Further work is necessary with regard to the correction of the NCR data in terms of understanding of the behaviour of the sensor, data calibration, and comparison to borehole data. Furthermore, it is planned to undertake point measurements of the magnetic susceptibility in selected intervals to

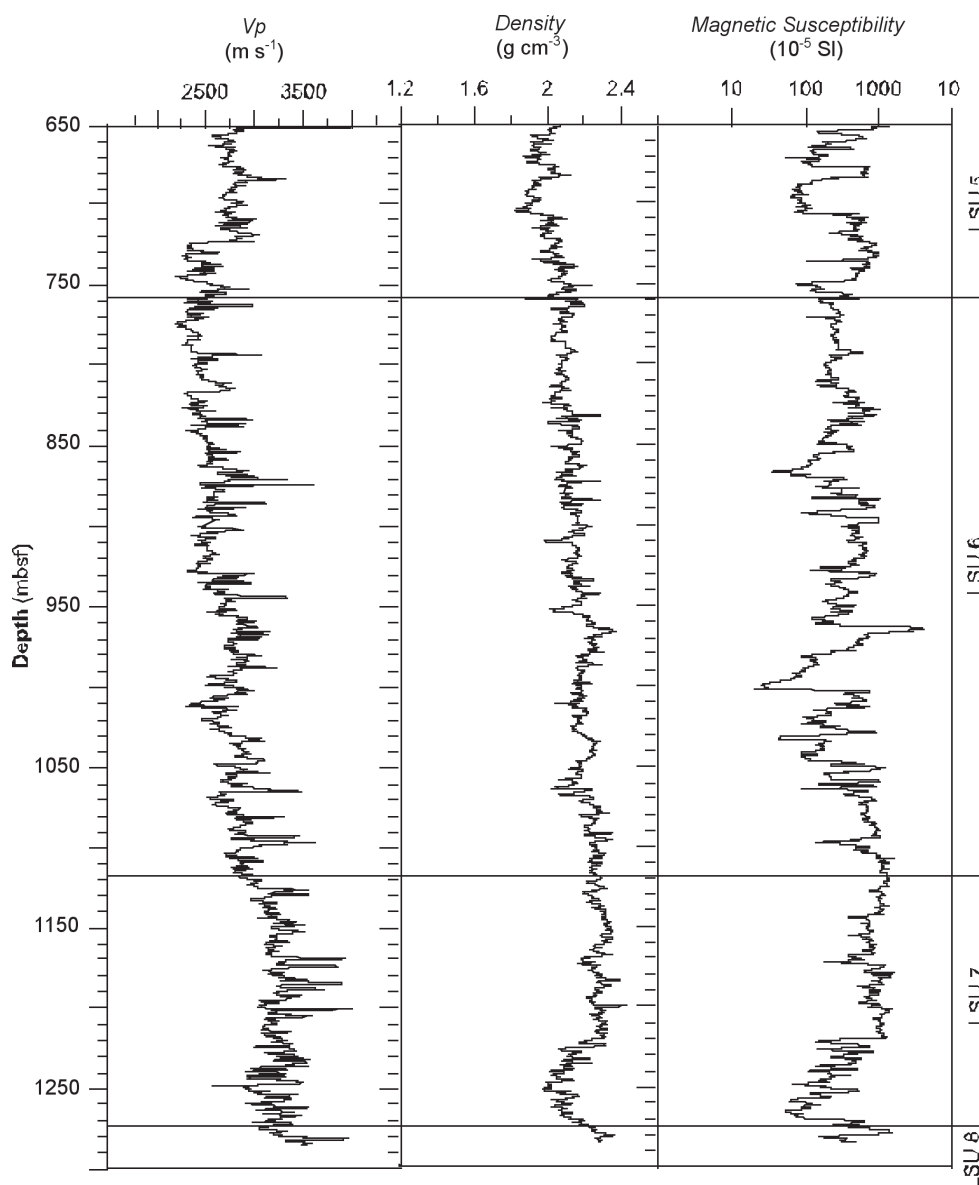


Fig. 8 – Summary logs of Vp, WBD, and MS (cumulative data smoothed over 50 data points) from 650 to 1285 mbsf subdivided into lithostratigraphic units (LSU).

improve vertical resolution and to account for the influence of clasts and bad core recovery in the variations within this parameter. We envisage a refinement of fractional porosities by grain densities determined from pycnometer measurements followed by analysis of compaction trends and porosity-velocity relationships. Additionally, intensive work on the analysis of the transmission seismograms will be carried out with the attempt to establish a relationship between their spectral amplitudes and grain-size composition (Breitzke et al. 1996) and – where applicable – other effects such as of volcanic petrology and cementation.

*Acknowledgements*—The ANDRILL project is a multinational collaboration between the Antarctic programmes of Germany, Italy, New Zealand and the United States. Antarctica New Zealand is the project operator and developed the drilling system in collaboration with Alex Pyne at Victoria University of Wellington and Webster Drilling

and Enterprises Ltd. Antarctica New Zealand supported the drilling team at Scott Base; Raytheon Polar Services Corporation supported the science team at McMurdo Station and the Crary Science and Engineering Laboratory. The ANDRILL Science Management Office at the University of Nebraska-Lincoln provided science planning and operational support. Scientific studies are jointly supported by the US National Science Foundation, NZ Foundation for Research, Science and Technology and the Royal Society of NZ Marsden Fund, the Italian Antarctic Research Programme, the German Research Foundation (DFG) and the Alfred Wegener Institute for Polar and Marine Research.

#### REFERENCES

Barrett P., Carter L., Dunbar G.B., Dunker E., Giorgetti G., Niessen F., Nixdorf U., Payne A.R., Riesselman C. & Robinson N., 2004. Oceanography and Sedimentation beneath the McMurdo/Ross Ice Shelf in Windless Bight, School of Earth Sciences, Victoria University Antarctic Research Centre, *Antarctic Data Series*, **25**.

- Best A.I. & Gunn D.E., 1999. Calibration of Marine Sediment Core Loggers for Quantitative Acoustic Impedance Studies. *Marine Geology*, **160**, 137-146.
- Breitzke M., Grobe H., Kuhn G., & Müller P., 1996. Full Waveform Ultrasonic Transmission Seismograms: A Fast New Method for the Determination of Physical and Sedimentological Parameters of Marine Sediment Cores. *J. Geophys. Res.*, **101**, B10, 22,123-22,141.
- Bücker C.J., Jarrard R.D., Niessen F., & Wonik T., 2001. Statistical Analysis of Wireline Logging Data of Cape Roberts Borehole CRP-3 (Antarctica). *Terra Antartica*, **8**, 491-506.
- Cape Roberts Science Team, 1998. Initial Report on CRP-1, Cape Roberts Project, Antarctica. *Terra Antartica*, **5**(1), 187 p.
- Cape Roberts Science Team, 1999. Initial Report on CRP-2/2A, Cape Roberts Project, Antarctica. *Terra Antartica*, **6**(1/2), 173 p.
- Cape Roberts Science Team, 2000. Initial Report on CRP-3, Cape Roberts Project, Antarctica. *Terra Antartica*, **7** (1/2), 209 p.
- Claps M., Niessen F., & Florindo F., 2000. High-Frequency Analysis of Physical Properties from CRP-2/2A, Victoria Land Basin, Antarctica and Implication for Sedimentation Rate, *Terra Antartica*, **7**(3), 379-388.
- Falconer T., Pyne A., Levy R., Olney M., Curren M., & the ANDRILL-MIS Science Team, this volume. Operations Overview for the ANDRILL McMurdo Ice Shelf Project, Antarctica. *Terra Antartica*.
- Henry S.A., Bücker C.J., Bartek L.R., Bannister S., Niessen F., & Wonik T., 2000. Correlation of Seismic Reflectors with CRP-2/2A, Victoria Land Basin, Antarctica, *Terra Antartica*, **7**(3), 221-230.
- Henry S.A., Bücker C.J., Niessen F., & Bartek L.R., 2001. Correlation of Seismic Reflections with Drillhole CRP-3, Victoria Land Basin, Antarctica, *Terra Antartica*, **8**(3), 127-136.
- Jarrard R.D., Niessen F., Brink J.D., & Bücker C., 2000. Effects of Cementation on Velocities of Siliclastic Sediments, *Geophys. Res. Lett.*, **27/5**, 593-596.
- Krissek L., Browne G., Carter L., Cowan E., Dunbar G., McKay R., Naish T., Powell R., Reed J., Wilch T., & the ANDRILL-MIS Science Team, this volume. Sedimentology and Stratigraphy of the AND-1B core, ANDRILL McMurdo Ice Shelf Project, Antarctica. *Terra Antartica*.
- Morin R., Williams T., Henry S., Crosby T., Hansaraj D., & the ANDRILL-MIS Science Team, this volume. Downhole Measurements of the AND-1B Borehole, ANDRILL McMurdo Ice Shelf Project, Antarctica. *Terra Antartica*.
- Naish T., Powell R., Levy R., & the ANDRILL-MIS Science Team, this volume. Background to the ANDRILL McMurdo Ice Shelf Project, Antarctica. *Terra Antartica*.
- Naish T.R., Woolfe K.J., Barrett P.J., Wilson G.S., Atkins C., Bohaty S.M., Bücker C.J., Claps M., Davey F.J., Dunbar G.B., Dunn A.G., Fielding C.R., Florindo F., Hannah M.J., Harwood D.M., Henry S.A., Krissek L.A., Lavelle M., Meer J. van der, McIntosh W.C., Niessen F., Passchier S., Powell R.D., Roberts A.P., Sagnotti L., Scherer R.P., Strong C.P., Talarico F., Verosub K.L., Villa G., Watkins D.K., Webb P.-N., & Wonik T., 2001. Orbitally Induced Oscillations in the East Antarctic Ice Sheet at the Oligocene/Miocene Boundary, *Nature*, **413**, 719-723.
- Niessen F. & Jarrard R.D., 1998. Velocity and Porosity of Sediments from the CRP-1 Drillhole, Ross Sea, Antarctica. *Terra Antartica*, **5**, 311-318.
- Niessen F., Jarrard R.D., & Bücker C., 1998. Log-Based Physical Properties of the CRP-1 Core, Ross Sea, Antarctica. *Terra Antartica*, **5**, 299-310.
- Niessen F., Kopsch K., & Polozek K., 2000. Velocity and Porosity from CRP-2/2A Core Logs, Victoria Land Basin, Antarctica, *Terra Antartica*, **7**(3), 241-254.
- Weber M.E., Niessen F., Kuhn G., & Wiedicke M., 1997. Calibration and Application of Marine Sedimentary Physical Properties using a Multi-Sensor Core Logger. *Marine Geology*, **136**, 151-172.
- Wilson G., Florindo F., Sagnotti L., & Ohneiser C., this volume. Paleomagnetism of the AND-1B Core, ANDRILL McMurdo Ice Shelf Project, Antarctica. *Terra Antartica*.
- Wilson G., Levy R., Browne G., Cody R., Dunbar N., Florindo F., Henry S., Graham I., McIntosh W., McKay R., Naish T., Ohneiser C., Powell R., Ross J., Sagnotti L., Scherer R., Sjunneskog C., Strong C.P., Taviani M., Winter D. & the ANDRILL-MIS Science Team, this volume. Preliminary Integrated Chronostratigraphy of the AND-1B Drillcore, ANDRILL McMurdo Ice Shelf Project, Antarctica. *Terra Antartica*.